View metadata, citation and similar papers at core.ac.uk
brought to you by CORE
provided by Digital.CSIC

Kinetic models comparison for non-isothermal steam gasification of coal-biomass blend chars

J. Fermoso, M.V. Gil, C. Pevida, J.J. Pis, F. Rubiera*

Instituto Nacional del Carbón, CSIC, Apartado 73, 33080 Oviedo, Spain

Abstract

The non-isothermal thermogravimetric method (TGA) was applied to a bituminous coal (PT), two types of biomass, chestnut residues (CH) and olive stones (OS), and coal-biomass blends in order to investigate their thermal reactivity under steam. Fuel chars were obtained by pyrolysis in a fixed-bed reactor at a final temperature of 1373 K for 30 min. The gasification tests were carried out by thermogravimetric analysis from room temperature to 1373 K at heating rates of 5, 10 and 15 K min^{-1}. After blending, no significant interactions were detected between PT and CH during co-gasification, whereas deviations from the additive behaviour were observed in the PT-OS blend. However, for the two coal-biomass blends, the gasification behaviour resembled that of the individual coal, as this component constituted the larger proportion of the blend. The temperature-programmed reaction (TPR) technique was employed at three different heating rates to analyze noncatalytic gas-solid reactions. Three *n*th-order representative gas-solid models, the volumetric model (VM), the grain model (GM) and the random pore model (RPM) were applied in order to describe the reactive behaviour of the chars during steam gasification. From these models, the kinetic parameters were determined. The best model for describing the reactivity of the PT, PT-CH and PT-OS samples was the RPM model. VM was the model that best fitted the CH sample, whereas none of the models was suitable for the OS sample.

Keywords: non-isothermal TG, coal, biomass, char gasification, kinetic models

1. Introduction

With the EU announcing that it intends to supply 20% of its overall energy needs from renewable sources by 2020, interest in biomass as a renewable source is growing [1].

* Corresponding author. Tel.: +34 985 118 975; Fax: +34 985 297 662

E-mail address: frubiera@incar.csic.es (F. Rubiera)

The traditional energy use of biomass is combustion, but more modern options are possible. Biomass can be pyrolysed or gasified to produce a liquid fuel or a gas fuel such as methane, hydrogen and carbon monoxide.

Coal gasification is an efficient technology for coal utilization due to its high carbon conversion and its contribution to the reduction of air pollutant emissions [2]. Biomass gasification is also one of the most promising technologies because of its ability to rapidly convert large amounts and various kinds of biomass into easily storable and transportable gas or liquid fuel [3,4]. In gasification processes, biomass reacts with steam and air at high temperatures to form a gas mixture of carbon monoxide, hydrogen and methane, together with carbon dioxide and nitrogen, which is suitable for direct use in combined-cycle gas turbine systems or which can be used as syngas. This syngas has a high calorific value and can replace fossil fuels in high efficiency power generation, heat, combined heat and power applications and in the production of liquid fuels and chemicals via synthesis gas [5].

Hydrogen is considered as the major energy carrier of the future, so an increase in the demand for hydrogen can be expected. Nowadays, there is increasing interest in lower cost fuels that can be used to produce mixtures of hydrogen and carbon monoxide by means of gasification. Co-gasification of coal with other less carbon containing fuels, such as biomass, offers the advantage of a reduction in CO_2 emissions, and even a net reduction, if CO_2 capture is incorporated as part of the process [6].

Gasification can be divided into two main stages: pyrolysis and the subsequent gasification of the remaining char, the latter stage being the controlling step of the overall process. For these reasons, knowledge about the reactivity of chars, and their variation as reaction progresses, and about the kinetics of the gasification process, is fundamental for the design of gasification reactors, since it is char gasification that determines the final conversion achieved in the process [7].

Thermogravimetric analysis (TGA) is a common technique used to investigate thermal events during the combustion, pyrolysis and gasification of solid raw materials, such as coal, wood, etc. [8-12]. Moreover, quantitative methods can be applied to TGA curves in order to obtain kinetic parameters of the thermal events. Miura and Silveston [13] demonstrated the validity of the TPR technique for the analysis of noncatalytic gas-solid reactions. This technique has been applied to the analysis of coal gasification because it

appears to provide more kinetic information than what is obtainable from the same number of experiments performed at constant temperature. Kasaoka et al. [14] also stated that in an isothermal experiment, a tedious repetition of experimental runs is required to determine the kinetic parameters of the Arrhenius equation. A precise knowledge of the kinetic characteristics of the gasification process is essential for understanding and modelling gasification at industrial scale.

There are several studies on coal gasification kinetics [15-17] and some on biomass gasification kinetics [4,18-19]. However, coal-biomass blends gasification has hardly been studied at all. The aim of the present work was to study the steam gasification reactivity and kinetic behaviour of a bituminous coal and two types of biomass (residues of chestnut and olive stones), as well as coal-biomass blends. For this purpose, the temperature-programmed reaction (TPR) technique at three different heating rates was used. Three mathematical models were used to determine the kinetic parameters which best represent the gasification characteristics of the chars from the coal-biomass blends under a nitrogen-steam mixture atmosphere.

2. Experimental

2.1. Fuel samples

The raw materials used in this work were a Spanish bituminous coal from Puertollano (Spain) with a high ash content (PT) and two types of biomass: residues of chestnut (CH) and olive stones (OS). These materials were ground, sieved and the resulting 1-2 mm size fraction was used for the pyrolysis tests. The volatile matter contents of the raw samples were 23.8, 80.7 and 82.4 wt.% (dry basis) for PT, CH and OS, respectively. The ash composition of the raw samples is given in Table 1.

2.2. Char preparation

The chars were prepared by devolatilizing the raw fuels in a quartz fixed bed reactor (20 mm internal diameter, 455 mm length) heated by an electric furnace under a stream of nitrogen (150 Nml min^{-1}). A thermocouple in contact with the sample bed was used to control the devolatilisation temperature. The samples were subjected to a heating rate of 15 K min^{-1} up to 1373 K and held at this temperature for 30 min. Afterwards, the chars were cooled down under a flow of nitrogen to room temperature. The char

samples were ground and sieved to a size of <150 μm for the gasification experiments. Moreover, two blends composed of 70 wt% of coal and 30 wt% of biomass (PT-CH and PT-OS) were prepared. The proximate and ultimate analyses of the char samples are given in Table 1. The PT, CH and OS samples underwent the loss of 94.5, 91.0 and 90.3 % of their volatile matter, respectively, during the pyrolysis process.

2.3. Gasification tests

Thermogravimetric analysis is a technique that is frequently used to determine the kinetic parameters of carbonaceous materials [20-22]. A thermobalance (Setaram TAG24) was used for the gasification tests which were conducted at atmospheric pressure. Approximately 5 mg of sample was deposited in a crucible of 2 mm height with a circular base of 5 mm diameter. A thermocouple was placed close to the platinum basket to monitor temperature and to close the oven control loop. In this work, all the experiments were performed under non-isothermal conditions at three different heating rates: 5, 10 and 15 K min^{-1}.

The total flow rate of the reactive gas introduced into the thermobalance during the gasification experiments was 150 NmL min^{-1}, comprising 30% of steam and 70% of N_2. The steam generator consisted of a CEM® (Controlled Evaporator and Mixer), in which water and N_2 were mixed and heated up to the desired temperature (423 K). Liquid and mass flow controllers were used to control the flow rates of water and nitrogen in order to ensure that the desired steam concentration remained constant.

Duplicate experiments for each test were performed in order to test the reproducibility of the results. The char conversion, X, and the reaction rate, dX/dt, were represented as a function of temperature, T.

3. Kinetic models

A general kinetic expression for the overall reaction rate in gas-solid reactions is written as follows [23]:

$$\frac{dX}{dt} = k\left(P_g, T\right) f(X) \tag{1}$$

where k is the apparent gasification reaction rate, which includes the effect of temperature (T) and the effect of the gasifying agent partial pressure (P_g), and $f(X)$

describes the changes in the physical or chemical properties of the sample as the gasification proceeds. Assuming that the partial pressure of the gasifying agent remains constant during the process, the apparent gasification reaction rate is dependent on the temperature and can be expressed using the Arrhenius equation, which is written as:

$$k = k_0 e^{-E/RT} \tag{2}$$

where k_0 and E are the pre-exponential factor and activation energy, respectively.

In this work, three *n*th-order models were applied in order to describe the reactivity of the chars studied: the volumetric model (VM), the grain model (GM) and the random pore model (RPM). These models give different formulations of the term *f(X)*.

The VM assumes a homogeneous reaction throughout the particle and a linearly decreasing reaction surface area with conversion [24]. The overall reaction rate is expressed by:

$$\frac{\mathrm{d}X}{\mathrm{d}t} = k_{\mathrm{VRM}}(1-X) \tag{3}$$

The GM or shrinking core model, proposed by Szekely and Evans [25], assumes that a porous particle consists of an assembly of uniform nonporous grains and the reaction takes place on the surface of these grains. The space between the grains constitutes the porous network. The shrinking core behaviour applies to each of these grains during the reaction. In the regime of chemical kinetic control and, assuming the grains have a spherical shape, the overall reaction rate is expressed in these models as:

$$\frac{\mathrm{d}X}{\mathrm{d}t} = k_{\mathrm{GM}}(1-X)^{2/3} \tag{4}$$

This model predicts a monotonically decreasing reaction rate and surface area because the surface area of each grain is receding during the reaction.

The RPM model considers the overlapping of pore surfaces, which reduces the area available for reaction [26]. The basic equation for this model is:

$$\frac{\mathrm{d}X}{\mathrm{d}t} = k_{\mathrm{RPM}}(1-X)\sqrt{1-\psi \ln(1-X)} \tag{5}$$

This model is able to predict a maximum for the reactivity as the reaction proceeds, as it considers the competing effects of pore growth during the initial stages of gasification, and the destruction of the pores due to the coalescence of neighbouring pores during the

reaction. The RPM model contains two parameters, the reaction rate constant, k_{RPM}, and ψ, which is a parameter related to the pore structure of the unreacted sample (X=0):

$$\psi = \frac{4\pi L_0 (1-\varepsilon_0)}{S_0^2} \tag{6}$$

where S_0, L_0 and ε_0 represent the pore surface area, pore length, and solid porosity, respectively.

According to Miura and Silveston [13], the determination of the kinetic parameters from a single TPR run may lead to unreliable rate parameters and, furthermore, the fitting of data by a model may not validate the model if just one TPR run is used. These authors claimed that at least three TPR runs at different heating rates are required to estimate reliable rate parameters. Therefore, in this study the kinetic parameters were determined from three TPR runs, each one performed at a different heating rate. The nonlinear least-squares method was employed to fit the experimental data of dX/dt vs. temperature, T, to the three models, Equations (3)-(5), and to estimate the k_0 and E values that minimize the objective function, OF:

$$\mathrm{OF} = \sum_{i=1}^{N} \left(\left(\frac{\mathrm{d}X}{\mathrm{d}t} \right)_{\mathrm{exp},i} - \left(\frac{\mathrm{d}X}{\mathrm{d}t} \right)_{\mathrm{calc},i} \right)^2 \tag{7}$$

where $(\mathrm{d}X/\mathrm{d}t)_{\mathrm{exp},i}$ is the experimental point corresponding to the i^{th} temperature, T_i, $(\mathrm{d}X/\mathrm{d}t)_{\mathrm{calc},i}$ is the value calculated at T_i, and N is the number of data points. The best fitting kinetic parameters were chosen from the best R^2 value obtained from those results which proved to be statistically significant.

The non-isothermal thermogravimetric method or temperature-programmed reaction (TPR) technique involves heating the samples at a constant rate, a. The temperature, T, is related to time, t, by:

$$T = T_0 + at \tag{8}$$

where T_0 is the temperature at which heating is started, which can be set equal to 0 provided that T_0 is low enough for the reaction rate to be practically zero when heating is initiated.

By means of Equation (8), Equation (3) can be integrated to give:

$$X = 1 - \exp\left(-\frac{k_0 E}{aR} p(u) \right) \tag{9}$$

where

$$p(u) = \frac{e^{-u}}{u} - \int_{X}^{\infty} \frac{e^{-u}}{u} du \tag{10}$$

$$u = \frac{E}{RT} \tag{11}$$

From the literature, several proposed approximations for $p(u)$ can be found. In this study the one employed has been [13,27,28]:

$$p(u) = \frac{e^{-u}}{u^2} \tag{12}$$

This approximation is valid for $u > 10$, which is totally fulfilled by these fuels when gasified by steam. Equation (9) can then be written as:

$$X = 1 - \exp\left(-\frac{RT^2}{aE} k_0 e^{\frac{-E}{RT}} \right) \tag{13}$$

Similarly, Equations (4) and (5) can be integrated with the above approximation, to give Equations (14) and (15) respectively:

$$X = 1 - \left[1 - \frac{RT^2}{3aE} k_0 e^{\frac{-E}{RT}} \right]^3 \tag{14}$$

$$X = 1 - \exp\left[-\frac{RT^2}{aE} k_0 e^{\frac{-E}{RT}} \left(1 + \frac{\psi}{4} \left(\frac{RT^2}{aE} \right) k_0 e^{\frac{-E}{RT}} \right) \right] \tag{15}$$

Equations (13)-(15) are used to calculate 1-X introducing the previously estimated k_0 and E values. The 1-X calculation was performed in order to verify the reliability of the kinetic models and their capacity to describe not only the reaction rate, dX/dt, but also char conversion, X (or 1-X). By comparing the experimental and calculated 1-X and dX/dt values, the kinetic model may be further tested and verified. The deviation (DEV) between the experimental and calculated curves was calculated using the following expressions:

$$\mathrm{DEV}(1-X)(\%) = 100 \frac{\sqrt{\sum_{i=1}^{N} \frac{(1-X)_{\mathrm{calc},i} - (1-X)_{\mathrm{exp},i}}{N}}}{\max(1-X)_{\mathrm{exp}}} \tag{16}$$

$$\mathrm{DEV}\left(\frac{\mathrm{d}X}{\mathrm{d}t}\right)(\%) = 100\frac{\sqrt{\sum_{i=1}^{N}\frac{\left(\frac{\mathrm{d}X}{\mathrm{d}t}\right)_{\mathrm{calc},i}-\left(\frac{\mathrm{d}X}{\mathrm{d}t}\right)_{\mathrm{exp},i}}{N}}}{\max\left(\frac{\mathrm{d}X}{\mathrm{d}t}\right)_{\mathrm{exp}}} \quad (17)$$

where $(1\text{-}X)_{\mathrm{calc},i}$ and $(1\text{-}X)_{\mathrm{exp},i}$ represent the calculated and experimental data of 1-X, $(\mathrm{d}X/\mathrm{d}t)_{\mathrm{calc},i}$ and $(\mathrm{d}X/\mathrm{d}t)_{\mathrm{exp},i}$ represent the calculated and experimental data of $\mathrm{d}X/\mathrm{d}t$, N is the number of data points, and $\max(1\text{-}X)_{\mathrm{exp}}$ and $\max(\mathrm{d}X/\mathrm{d}t)_{\mathrm{exp}}$ are the highest absolute values of the experimental curves.

4. Results and discussion

4.1. Thermogravimetric characteristics of the char samples under a steam atmosphere

The heating rate had a marked influence on the gasification reactivity of the fuel char, independently of its nature. Figure 1 shows the experimental reactivity data of the individual fuel chars (PT, CH and OS) and the coal-biomass char blends (PT-CH and PT-OS) studied in this work as a function of reaction temperature at three different heating rates (5, 10 and 15 K min^{-1}). Table 2 shows the initial, peak and final temperatures corresponding to the experimental reactivity plots. From a qualitative point of view, all the curves presented a single peak, which corresponds to the maximum rate of mass loss, i.e., maximum reactivity. An increase in the heating rate hardly affected the initial reaction temperature (Table 2), which was considered in this work to be the temperature at which the rate of mass loss was 0.005 % s^{-1} [29]. However, the maximum peak height temperature was visibly displaced to higher values (Table 2). With the increasing heating rates, temperature increases faster and individual reactions do not have enough time to reach completion, or equilibrium, and they overlap with the adjacent higher temperature reaction. [30]. The gasification of the biomass chars starts at lower temperatures than that of the coal char (Table 2). With respect to the biomass samples, even though they have a similar composition, they show very different reactivities. The OS char started to react at temperatures approximately 50 K lower than those of CH. The biggest difference lies in the shape of the reactivity curves. They are much sharper in the case of the OS char. In addition, the maximum reaction rate values, which occur at lower temperatures (between 44 and 55 K), were nevertheless between 3 to 4 times higher than those of the CH char at the three heating

rates. Table 1 presents the ash elemental composition of the three fuels studied in this work, expressed as metallic oxides, and determined by atomic absorption spectrophotometry, except for Na and K, which were determined by atomic emission. In this table, it can be observed that, among the catalytically active elements that may be present in the mineral matter of biomass fuels, the potassium content of the olive stones (OS) is much higher than that of chestnut (CH), which might explain its much higher reactivity, as has been pointed out by other authors [31, 32]. Di Blasi [33] also observed a high reactivity in olive stones due to a catalytic effect associated to the high alkali content of the samples, especially potassium, during their combustion and gasification.

In the case of the two coal-biomass blends, PT-CH and PT-OS, the presence of biomass (30 wt.%) during the coal gasification displaced the initial reaction temperature to lower values with respect to those of the PT coal, this decrease reaching values of between 13 and 39 K in the case of the PT-CH blend, and between 22 and 40 K, in the PT-OS blend (Table 2). The maximum reaction rate temperature was also slightly displaced to lower values with respect to those of the PT coal, decreasing between 4 and 17 K for the PT-CH blend, and between 12 and 29 K in the case of the PT-OS blend (Table 2).

4.2. Interactions between the components of the blends

The theoretical and experimental dX/dt curves of the blends were compared in order to find out whether the components of the blends interacted during the gasification process. The theoretical dX/dt curves of the blends were calculated according to the additive rule of blends, i.e.:

$$(\mathrm{d}X/\mathrm{d}t)_{\mathrm{blend}} = x_1(\mathrm{d}X/\mathrm{d}t)_{\mathrm{coal}} + x_2(\mathrm{d}X/\mathrm{d}t)_{\mathrm{biomass}} \quad (18)$$

where $(\mathrm{d}X/\mathrm{d}t)_{\mathrm{coal}}$ and $(\mathrm{d}X/\mathrm{d}t)_{\mathrm{biomass}}$ are the reaction rate of the individual fuels, and x_1, x_2 are the proportions of coal and biomass in the blend, respectively.

In Figure 2 no significant deviations can be appreciated between the experimental and calculated dX/dt curves in the case of the PT-CH blend at the three heating rates. Therefore, no interaction could have taken place during the gasification process, reflecting the additive behaviour of this blend. This means that it should be possible to predict the experimental reactivity curve of the blend on the basis of the experimental reactivity curves of each individual component and their percentages in the blend. The absence of synergetic effects during the gasification process indicates that the

gasification reactions of the biomass were not significantly affected by the presence of coal, just as coal did not seem to be influenced by the presence of 30 wt% of biomass. Each component of the mixture behaved independently and did not interact with the other material.

Figure 2 also shows the experimental and calculated dX/dt curves in the case of the PT-OS blend during its gasification at three heating rates. As can be seen from the figure, the two components of the blend interacted strongly during the gasification process. According to the additive rule, the reactivity curve should present two peaks corresponding to the contribution of the maximum reactivity of each blended fuel. However, the shape of the experimental curve of the PT-OS blend presented a single peak, which resembled that of the coal char, i.e., the larger component. This indicates that the type of biomass added to the coal, when added in a proportion of 30%, has very little effect on the gasification of the blend. It also means that the gasification reactions of biomass OS were significantly affected by the presence of coal, whereas coal PT, was not apparently affected by the biomass. Nevertheless, the PT-OS curve was slightly displaced towards lower temperatures compared to that of the PT sample, due to the presence of the OS char, as a result of which reactivity in the blend increased. These deviations between the experimental and calculated dX/dt curves of the PT-OS blend can be attributed to the synergetic effects that occurred during the char gasification process.

Other authors [34-36] also observed a similar behaviour. Their coal-biomass blend curves resembled those of the coal sample, as this component was present in a larger proportion during the co-combustion of different coal and biomass blends. However, the maximum reaction rate values were also lower than those produced during coal gasification, as in the case of the individual biomasses.

Several authors have observed interactions between the components of coal and biomass blends [10,37], while others have reported additive behaviour [38-43].

4.3. Kinetic parameters

Table 3 shows the kinetic parameters (E, k_0 and ψ) determined from the data obtained at the three heating rates (5, 10 and 15 K min^{-1}) for all the char samples together with the coefficients of determination, R^2, for each model and char sample. R^2 shows the

variation in the dependent variable, dX/dt, which is explained by the model. Table 3 also presents the statistically significant model fittings. Fig. 1 shows, for the three heating rates, the experimental dX/dt data and the dX/dt curves calculated (Equations (3)-(5)) using the parameters obtained from the data at the three heating rates for the statistically significant models.

The RPM model fits the experimental data better than the other two models for coal PT (R^2 = 0.996), PT-CH (R^2 = 0.994) and the PT-OS (R^2 = 0.986) char samples, since it displayed a significant fit and has the highest R^2 value (Table 3). In the case of the PT-OS sample, the R^2 value was very similar in the case of the VM and RPM models (see Fig. 1). This is due to the ψ value being very close to zero and when this occurs, the RPM model predicts a nearly constant decrease in reactivity with conversion, as does the VM model. The CH sample fitted the VM model (R^2 = 0.989) better, since in the case the RPM model, the fit was not significant.

Kajitani et al. [44] also described the gasification reaction of coal chars using the random pore model. Okumura et al. [45] found that the random pore model was more appropriate than the volume reaction model for describing the gasification reaction of biomass char. Matsumoto et al. [4] concluded that the random pore model was the one that best explained the biomass char gasification reaction in their experiments with wood, bark and grass.

On the other hand, none of the models could be satisfactorily fitted to the data of the OS sample. As previously mentioned, the OS char presented an extremely high reactivity, probably caused by the strong catalytic effect of indigenous alkali. This may be why the reactivity of OS cannot be described properly with the models used in this work, since these only take into account structural changes during the gasification process.

The conversion, 1-X, of the chars during gasification was calculated (Equations (13)-(15)) by using the kinetic parameters estimated from data at the three heating rates (Table 3). Fig. 3 shows, for the three heating rates, the experimental 1-X data and the 1-X curves calculated from the statistically significant models. In order to quantify the errors produced by the kinetic models in predicting the values of conversion, the experimental and calculated 1-X values were compared by calculating the deviation (DEV) between the experimental and calculated curves using Equation (16). The same procedure was applied to the dX/dt curves using Equation (17). The results obtained

from the significant models for all the char samples are summarised in Table 4. The lowest deviation from the calculated values of the reaction rates was obtained using the RPM model for the PT, PT-CH and PT-OS char samples and the VM model for the CH char sample. In relation to the conversion calculated values, the best ones were obtained using the RPM model for the PT and PT-CH char samples and the VM model for the CH and PT-OS char samples. Again this shows the similarity of fit between the VM and RPM models in the case of the PT-OS sample.

In agreement with other authors, Bhat et al. [18] claimed that the activation energies for the char gasification reactions of coal and biomass lie in the 142-360 kJ mol^{-1}range. In this study, using the models with the best fit, the activation energy for coal PT, was 259 kJ mol^{-1}, similar to that of the CH sample. Both blends also showed similar activation energy values.

In a previous study [46], a kinetic analysis of the steam gasification of the PT, CH and OS char samples was carried out at constant temperature. The results obtained using the TPR technique were then compared with those obtained from experiments performed at constant temperature. From the isothermal gasification experiments, it was concluded that the best model for describing the behaviour of the PT and CH samples was RPM, whereas the behaviour of OS was not described satisfactorily by any of the three models. However, in the case of the CH char sample, the deviation between the experimental and theoretical dX/dt data for the RPM and VM models was very close (7.7% and 8.4% respectively) and the kinetic parameters were also similar. Therefore, the two techniques were compared using the parameters estimated by means of the RPM model for the PT char sample and by the VM model for CH char sample. The OS char sample was not included in this comparison because none of the models was found to be statistically significant with the TPR technique. The values of $k_0e^{-E/RT}$ were calculated and plotted on an Arrhenius diagram using the kinetic parameters in Table 3 (Fig. 4) and then compared with those obtained in the isothermal experiments [46]. A good agreement can be observed between the $k_0e^{-E/RT}$ values estimated by both methods, indicating that the TPR technique provides reliable kinetics parameters when data from the three heating rates are used, in agreement with Miura and Silveston [13].

5. Conclusions

The chars from a bituminous coal (PT) and two types of biomass, residues of chestnut (CH) and olive stones (OS), as well as coal-biomass blends, were gasified in a thermobalance at atmospheric pressure in order to investigate their thermal reactivity under a nitrogen-steam atmosphere. No significant interactions were detected between the components in the PT-CH blend during co-gasification, whereas noticeable deviations from the expected behaviour were observed in the PT-OS blend. However, for both coal-biomass blends, gasification behaviour resembled that of the individual coal, which was the main component in the blend.

The temperature-programmed reaction technique employed in the analysis of noncatalytic gas-solid reactions was applied at three different heating rates in order to estimate the kinetic parameters which best describe the reactive behaviour of the chars during steam gasification. The best model for describing the char steam gasification of the coal and coal-biomass blends was the random pore model. Steam gasification of the chestnut char was best described by the volumetric model, whereas that of the olive stones was not satisfactorily predicted by any of the studied models.

Acknowledgements

This work was carried out with financial support from the Spanish MICINN (Project PS- 120000-2006-3, ECOCOMBOS), and co-financed by the European Regional Development Fund, ERDF.

References

[1] European Commission, Directive 2009/28/EC. Official Journal of the European Union (2009) L 140/16-162.

[2] C. Higman, M. van der Burgt, Gasification, second ed., Elsevier Inc., USA, Burlington, USA, 2008.

[3] A. Gómez-Barea, L.F. Vilches, C. Leiva, M. Campoy, C. Fernández-Pereira, Plant optimisation and ash recycling in fluidised bed waste gasification, Chem. Eng. J. 146 (2009) 227–236.

[4] K. Matsumoto, K. Takeno, T. Ichinose, T. Ogi, M. Nakanishi, Gasification reaction kinetics on biomass char obtained as a by-product of gasification in an entrained-flow gasifier with steam and oxygen at 900-1000ºC, Fuel 88 (2009) 519-527.

[5] L. Yassin, P. Lettieri, S.J.R. Simons, A. Germanà, Techno-economic performance of energy-from-waste fluidized bed combustion and gasification processes in the UK context, Chem. Eng. J. 146 (2009) 315-327.

[6] V. Strezov, B. Moghtaderi, J.A. Lucas, Thermal study of decomposition of selected biomass samples, J. Therm. Anal. Calorim. 72 (2003) 1041-1048.
[7] C. Wolters, M. Kanaar, Update of Nuon Power Buggenum plant performance and fuel flexibility, in: Proceedings of the 2nd International Conference on Clean Coal Technologies for our future, Sardinia, Italy, 2005, pp. 1-20.
[8] J.J. Pis, G. de la Puente, E. Fuente, A. Morán, F. Rubiera, A study of the self-heating of fresh and oxidized coals by differential thermal analysis, Thermochim. Acta 279 (1996) 93-101.
[9] F. Rubiera, A. Arenillas, C. Pevida, R. García, J.J. Pis, K.M. Steel, J.W. Patrick, Coal structure and reactivity changes induced by chemical demineralisation, Fuel Process. Technol. 79 (2002) 273-279.
[10] G. Skodras, P. Grammelis, P. Basinas, Pyrolysis and combustion behaviour of coal-MBM blends, Bioresource Technol. 98 (2007) 1-8.
[11] C. Wang, F. Wang, Q. Yang, R. Liang, Thermogravimetric studies of the behavior of wheat straw with added coal during combustion, Biomass Bioenerg. 33 (2009) 50-56.
[12] A. Arenillas, F. Rubiera, J.J. Pis, J.M. Jones, A. Williams, The effect of the textural properties of bituminous coal chars on NO emissions, Fuel 78 (1999) 1779-1785.
[13] K. Miura, P.L. Silveston, Analysis of Gas-Solid Reactions by Use of a Temperature-Programmed Reaction Technique, Energ. Fuel. 3 (1989) 243-249.
[14] S. Kasaoka, Y. Sakata, M. Shimada, T. Matsutomi, A new kinetic model for temperature programed thermogravimetry and its applications to the gasification of coal chars with steam and carbon dioxide, J. Chem. Eng. Jpn. 18 (1985) 426-432.
[15] R.C. Everson, H.W.J.P. Neomagus, R. Kaitano, R. Falcon, V. M. du Cann, Properties of high ash coal-char particles derived from inertinite-rich coal: II. Gasification kinetics with carbon dioxide, Fuel 87 (2008) 3403-3408.
[16] H. Liu, C. Luo, S. Kato, S. Uemiya, M. Kaneko, T. Kojima, Kinetics of CO_2/Char gasification at elevated temperatures. Part I: Experimental results, Fuel Process. Technol. 87 (2006) 775-781.
[17] S. Wu, J. Gu, L. Li, Y. Wu, J. Gao, The reactivity and kinetics of Yanzhou coal chars from elevated pyrolysis temperatures during gasification in steam at 900-1200ºC, Process Saf. Environ. Protect. 84 (2006) 420-428.
[18] A. Bhat, J.V.R. Bheemarasetti, T.R Rao, Kinetics of rice husk char gasification, Energ. Convers. Manage. 42 (2001) 2061-2069.
[19] J. Fermoso, C. Stevanov, B. Moghtaderi, B. Arias, C. Pevida, M.G. Plaza, F. Rubiera, J.J. Pis, High-pressure gasification reactivity of biomass chars produced at different temperatures, J. Anal. Appl. Pyrol. 85 (2009) 287-293.
[20] A. Arenillas, F. Rubiera, C. Pevida, C.O. Ania, J.J. Pis, Relationships between structure and reactivity of carbonaceous materials, J. Therm. Anal. Calorim. 76 (2004) 593-602.
[21] H. Barkia, L. Belkbir, S.A.A Jayaweera, Kinetic studies of oxidation of residual carbon from Moroccan oil shale kerogens, J. Therm. Anal. Calorim. 86 (2006) 121-123.
[22] I.Y. Elbyli, S. Piskin, Combustion and pyrolysis characteristics of Tunçbilek lignite, J. Therm. Anal. Calorim. 83 (2006) 721-726.

[23] G.Q. Lu, D.D. Do, Comparison of structural models for high-ash char gasification, Carbon 32 (1994) 247-263.
[24] M. Ishida, C.Y. Wen, Comparison of zone-reaction model and unreacted-core shrinking model in solid-gas reactions – I Isothermal analysis, Chem. Eng. Sci. 26 (1971) 1031-1041.
[25] J. Szekely, J.W. Evans, A structural model for gas-solid reactions with a moving boundary, Chem. Eng. Sci. 25 (1970) 1091-1107.
[26] S.K. Bhatia, D.D. Perlmutter, A random pore model for fluid-solid reactions: I. Isothermal, kinetic control, AIChE J. 26 (1980) 379-386.
[27] V. Leroy, D. Cancellieri, E. Leoni, J.-L. Rossi, Kinetic study of forest fuels by TGA: Model-free kinetic approach for the prediction of phenomena, Thermochim. Acta 497 (2010) 1-6.
[28] K. Miura, H. Nakagawa, S. Nakai, S. Kajitani, Analysis of gasification reaction of coke formed using a miniature tubing-bomb reactor and a pressurized drop tube furnace at high pressure and high temperature, Chemical Engineering Science 59 (2004) 5261-5268.
[29] F. Rubiera, A. Arenillas, E. Fuente, N. Miles, J.J. Pis, Effect of the grinding behaviour of coal blends on coal utilisation for combustion, Powder Technol. 105 (1999) 351-356.
[30] S.St.J. Warne, Introduction to Thermal Analysis, in: E.L. Charsley, S.B. Warrington (Eds.), Thermal Analysis – Techniques and Applications, Royal Society of Chemistry, London, 1992, pp.1-16.
[31] P. Ollero, A. Serrera, R. Arjona, S. Alcantarilla, The CO_2 gasification kinetics of olive residue, Biomass Bioenerg. 24 (2003) 151-161.
[32] A. Gómez-Barea, P. Ollero, C. Fernández-Baco, Diffusional effects in CO_2 gasification experiments with single biomass particles. 1. Experimental Investigation, Energ. Fuel. 20 (2006) 2202-2210.
[33] C. Di Blasi, Combustion and gasification rates of lignocellulosic chars, Prog. Energ. Combust. 35 (2009) 121-140.
[34] E. Kastanaki, D. Vamvuka, A comparative reactivity and kinetic study on the combustion of coal-biomass char blends, Fuel 85 (2006) 1186-1193.
[35] H. Haykiri-Acma, S. Yaman, Effect of co-combustion on the burnout of lignite/biomass blends: A Turkish case study, Waste Manage. 28 (2008) 2077-2084.
[36] M. Otero, L.F. Calvo, M.V. Gil, A.I. García, A. Morán, Co-combustion of different sewage sludge and coal: A non-isothermal thermogravimetric kinetic analysis, Bioresource Technol. 99 (2008) 6311-6319.
[37] L. Zhou, Y. Wang, Q. Huang, J. Cai, Thermogravimetric characteristics and kinetic of plastic and biomass blends co-pyrolysis, Fuel Process. Technol. 87 (2006) 963-969.
[38] E. Biagini, F. Lippi, L. Petarca, L. Tognotti, Devolatilization rate of biomasses and coal-biomass blends: an experimental investigation, Fuel 81 (2002) 1041-1050.
[39] E. Kastanaki, D. Vamvuka, P. Grammelis, E. Kakaras, Thermogravimetric studies of the behavior of lignite-biomass blends during devolatilization, Fuel Process. Technol. 77-78 (2002) 159-166.
[40] D. Vamvuka, E. Kakaras, E. Kastanaki, P. Grammelis, Pyrolysis characteristics and kinetics of biomass residuals mixtures with lignite, Fuel 82 (2003) 1949-1960.

[41] D. Vamvuka, N. Pasadakis, E. Kastanaki, P. Grammelis, E. Kakaras, Kinetic modeling of coal/agricultural by-product blends,. Energ. Fuel. 17 (2003) 549-558.
[42] A.K. Sadhukhan, P. Gupta, T. Goyal, R.K. Saha, Modelling of pyrolysis of coal-biomass blends using thermogravimetric analysis, Bioresource Technol. 99 (2008) 8022-8026.
[43] W. Zhu, W. Song, W. Lin, Catalytic gasification of char from co-pyrolysis of coal and biomass, Fuel Process. Technol. 89 (2008) 890-896.
[44] S. Kajitani, S. Hara, H. Matsuda, Gasification rate analysis of coal char with a pressurized drop tube furnace, Fuel 81 (2002) 539-546.
[45] Y. Okumura, T. Hanaoka, K. Sakanishi, Effect of pyrolysis conditions on gasification reactivity of woody biomass-derived char, P. Combust. Inst. 32 (2009) 2013-2020.
[46] J. Fermoso, B. Arias, C. Pevida, M.G. Plaza, F. Rubiera, J.J. Pis, Kinetic models comparison for steam gasification of different nature fuel chars. J. Therm. Anal. Calorim. 91 (2008) 779-786.

Figure captions

Fig. 1. Experimental reaction rate curves of fuel chars and those calculated with three *n*th-order reaction models (VM, GM and RPM) using parameters determined from heating rates at 5, 10 and 15 K min^{-1}.

Fig. 2. Comparison between the experimental and calculated reaction rate curves, according to the additive rule from those of the individual components, during the non-isothermal (5, 10 and 15 K min^{-1}) steam gasification of coal-biomass blends.

Fig. 3. Experimental conversion curves of fuel chars and those calculated with three *n*th-order reaction models (VM, GM and RPM) using parameters determined from heating rates at 5, 10 and 15 K min^{-1}.

Fig. 4. Comparison between the apparent gasification reaction rates obtained from the TPR data (at heating rates of 5, 10 and 15 K min^{-1}) and data obtained from isothermal gasification experiments [46].

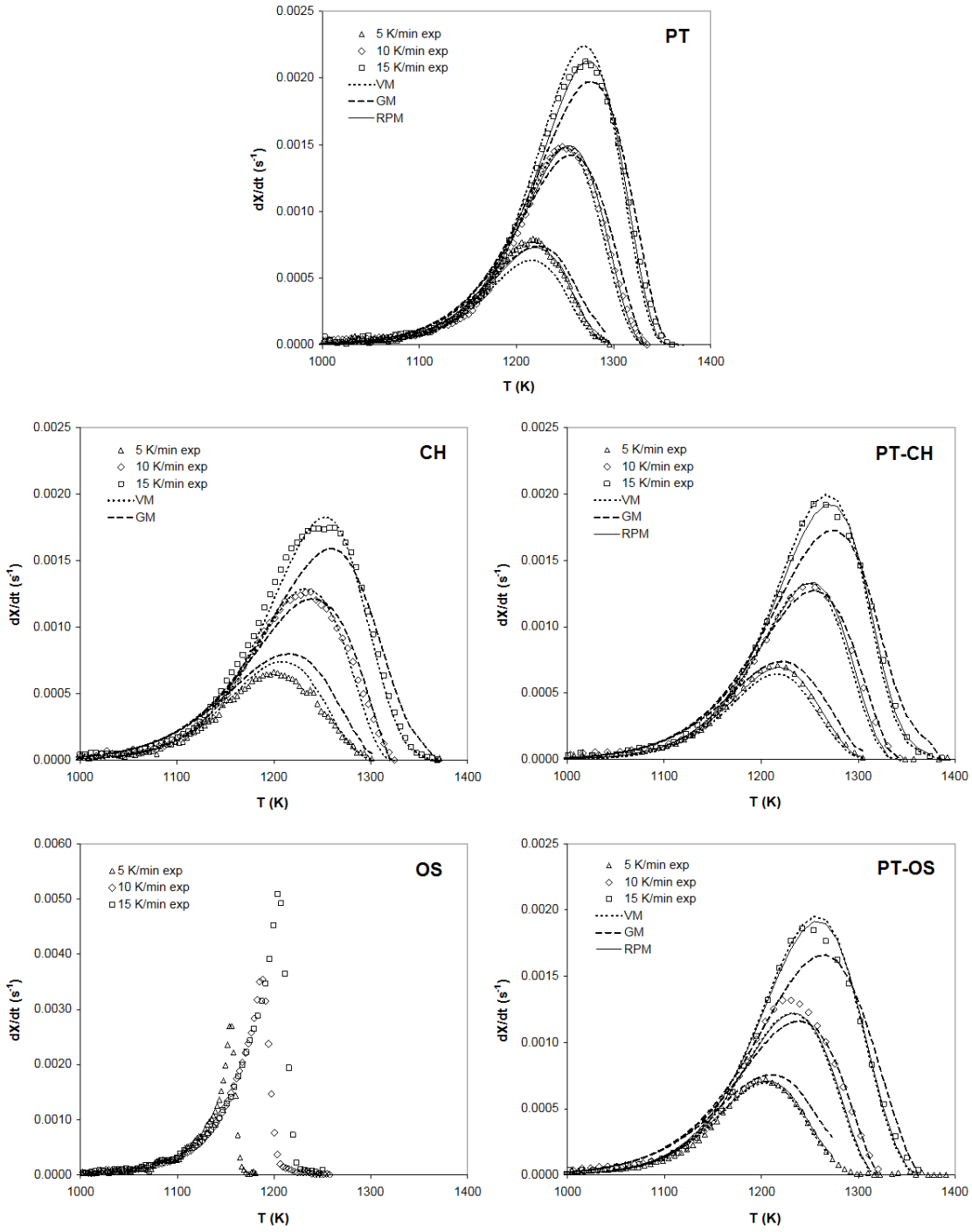

Fig. 1. Experimental reaction rate curves of fuel chars and those calculated with three *n*th-order reaction models (VM, GM and RPM) using parameters determined from heating rates at 5, 10 and 15 K min^{-1}.

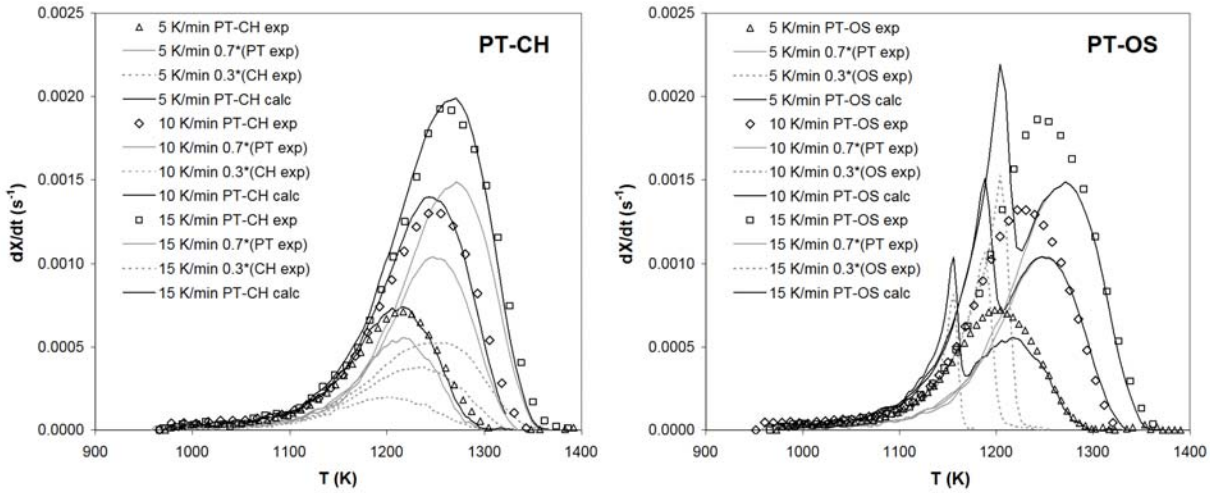

Fig. 2. Comparison between the experimental and calculated reaction rate curves, according to the additive rule from those of the individual components, during the non-isothermal (5, 10 and 15 K min^{-1}) steam gasification of coal-biomass blends.

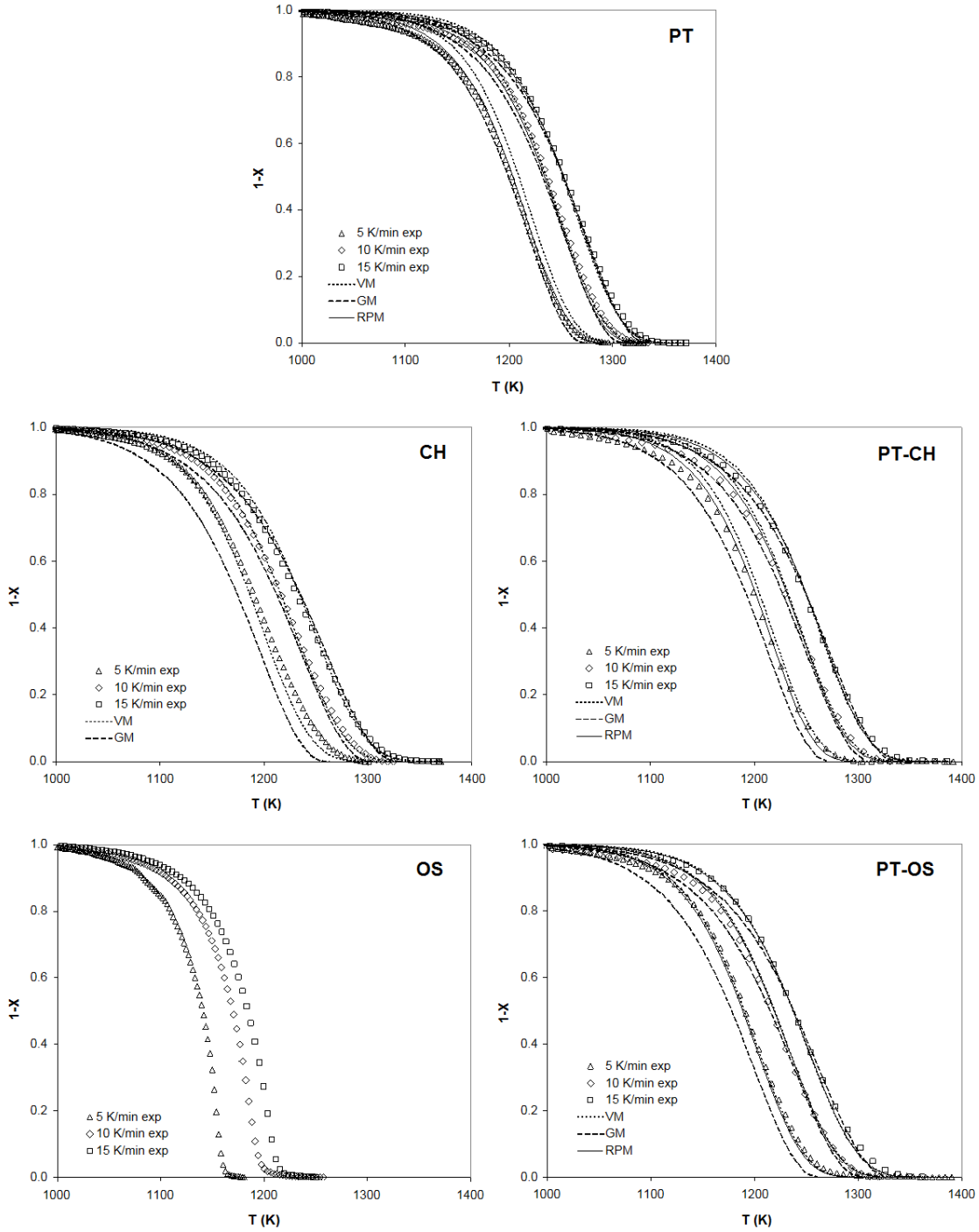

Fig. 3. Experimental conversion curves of fuel chars and those calculated with three *n*th-order reaction models (VM, GM and RPM) using parameters determined from heating rates at 5, 10 and 15 K min^{-1}.

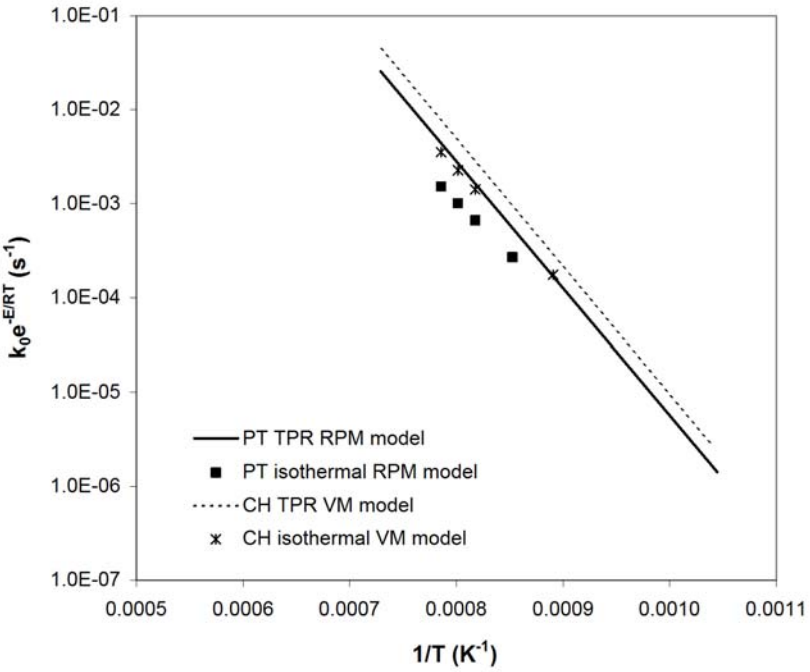

Fig. 4. Comparison between the apparent gasification reaction rates obtained from the TPR data (at heating rates of 5, 10 and 15 K min^{-1}) and data obtained from isothermal gasification experiments [46].

Table 1

Proximate and ultimate analyses of the char samples and elemental composition of the raw fuel ash

	Char sample								Ash content of raw sample						
	Proximate analysis (wt%, db)			Ultimate analysis (wt%, daf)					Metallic oxide (wt%)						
	Ash	VM	FC[a]	C	H	N	S	O[a]	SiO_2	Al_2O_3	Fe_2O_3	CaO	MgO	Na_2O	K_2O
PT	51.7	1.3	47.0	93.6	0.0	1.5	1.3	3.6	57.4	25.3	9.7	1.2	0.1	0.4	1.5
CH	3.0	7.3	89.7	97.2	0.0	0.6	0.0	2.2	40.0	12.4	6.70	21.5	3.5	0.9	6.7
OS	2.1	8.0	89.9	95.8	0.0	0.8	0.0	3.4	10.0	<3.0	4.2	26.5	4.1	0.5	28.3

[a] Calculated by difference; db: dry basis; daf: dry ash free basis

Table 2
Initial, peak and final temperatures of the reactivity plots

Sample	Temperature (K)		
	Initial	Peak	Final
5K/min			
PT	1081	1217	1288
CH	1060	1200	1294
OS	1032	1156	1170
PT-CH	1059	1217	1297
PT-OS	1058	1205	1284
10K/min			
PT	1055	1247	1329
CH	1048	1238	1320
OS	1019	1188	1224
PT-CH	1016	1243	1338
PT-OS	1015	1222	1320
15K/min			
PT	1068	1271	1351
CH	1045	1258	1349
OS	1010	1203	1244
PT-CH	1055	1254	1364
PT-OS	1042	1242	1356

Table 3
Kinetic parameters of the char samples during steam gasification determined with the TPR technique at three heating rates (5, 10 and 15 K min^{-1}) for three *n*th-order reaction models

Char	Volumetric model (VM)			Grain model (GM)			Random pore model (RPM)			
	E (kJ mol^{-1})	k_0 (s^{-1})	R^2	E (kJ mol^{-1})	k_0 (s^{-1})	R^2	E (kJ mol^{-1})	k_0 (s^{-1})	ψ	R^2
PT	304.2	1.99E+10	0.986*	236.8	2.10E+07	0.983*	258.5	1.79E+08	0.91	0.996*
CH	258.9	3.22E+08	0.989*	197.5	5.43E+05	0.951*	258.3	3.00E+08	0.01	0.989
OS	415.0	1.56E+16	0.694	376.6	5.44E+14	0.800	339.0	1.65E+10	2.7E+05	0.845
PT-CH	288.6	4.41E+09	0.990*	216.4	2.85E+06	0.968*	260.6	2.49E+08	0.42	0.994*
PT-OS	267.0	6.87E+08	0.985*	201.5	7.82E+05	0.946*	256.6	2.34E+08	0.13	0.986*

* Statistically significant (p-value<0.05)

Table 4
Deviation between the experimental and calculated conversion (1-*X*) and reaction rate (d*X*/d*t*) data

	DEV 1-*X* (%)			DEV *dX/dt* (%)		
	VM	GM	RPM	VM	GM	RPM
PT	2.59	2.58	1.29	2.85	3.19	1.63
CH	1.75	5.12	-	2.83	6.02	-
PT-CH	2.28	2.97	1.47	2.59	4.53	2.01
PT-OS	1.34	4.32	1.37	3.01	5.81	2.95